Hybrid polymeric hydrogels *via* peptide nucleic acid (PNA)/DNA complexation

Te-Wei Chu, Jiayue Feng, Jiyuan Yang, Jindřich Kopeček

PII: S0168-3659(15)30135-8
DOI: doi: 10.1016/j.jconrel.2015.09.035
Reference: COREL 7875

To appear in: *Journal of Controlled Release*

Received date: 21 July 2015
Revised date: 10 September 2015
Accepted date: 18 September 2015

Please cite this article as: Te-Wei Chu, Jiayue Feng, Jiyuan Yang, Jindřich Kopeček, Hybrid polymeric hydrogels *via* peptide nucleic acid (PNA)/DNA complexation, *Journal of Controlled Release* (2015), doi: 10.1016/j.jconrel.2015.09.035

Hybrid Polymeric Hydrogels *via* Peptide Nucleic Acid (PNA)/DNA Complexation

Te-Wei Chu[1], Jiayue Feng[2], Jiyuan Yang[1], and Jindřich Kopeček[1,3,*]

[1]Department of Pharmaceutics and Pharmaceutical Chemistry, [2]Department of Chemistry, and [3]Department of Bioengineering, University of Utah, Salt Lake City, UT 84112, USA

*To whom correspondence should be addressed (J. Kopeček):

University of Utah, Center for Controlled Chemical Delivery, 2030 East 20 South, Biopolymers Research Building, Room 205B, Salt Lake City, Utah 84112-9452, USA.

Phone: +1 (801) 581-7211; *Fax*: +1 (801) 581-7848

E-mail: jindrich.kopecek@utah.edu

Abstract

This work presents a new concept in hybrid hydrogel design. Synthetic water-soluble *N*-(2-hydroxypropyl)methacrylamide (HPMA) polymers grafted with multiple peptide nucleic acids (PNA) are crosslinked upon addition of the linker DNA. The self-assembly is mediated by the PNA–DNA complexation, which results in the formation of hydrophilic polymer networks. We show that the hydrogels can be produced through two different types of complexations. Type I hydrogel is formed *via* the PNA/DNA double-helix hybridization. Type II hydrogel utilizes a unique "P-form" oligonucleotide triple-helix that comprises two PNA sequences and one DNA. Microrheology studies confirm the respective gelation processes and disclose a higher critical gelation concentration for the type I gel when compared to the type II design. Scanning electron microscopy reveals the interconnected microporous structure of both types of hydrogels. Type I double-helix hydrogel exhibits larger pore sizes than type II triple-helix gel. The latter apparently contains denser structure and displays greater elasticity as well. The designed hybrid hydrogels have potential as novel biomaterials for pharmaceutical and biomedical applications.

Graphical Abstract:

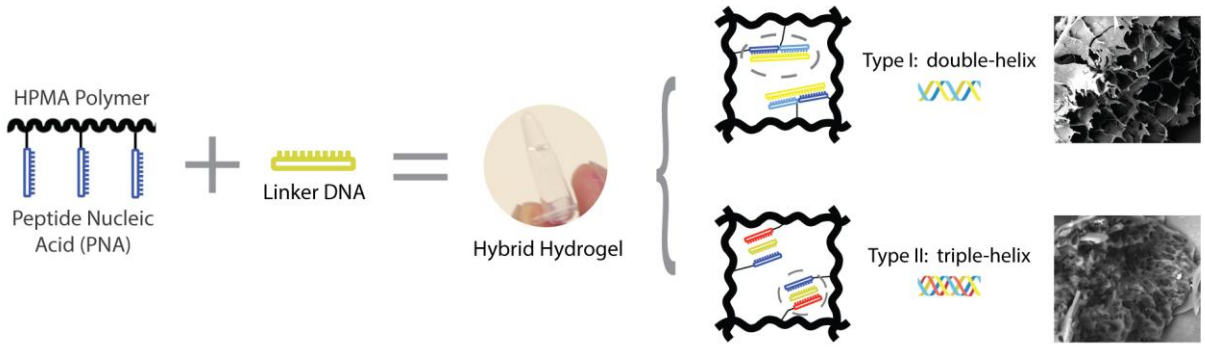

Keywords: hydrogel, self-assembly, peptide nucleic acid, HPMA polymer, DNA, P-form

1. Introduction

Hybrid hydrogels composed of synthetic and biological building blocks integrate the advantages of both components. For instance, the synthetic parts are beneficial for mass production and often provide mechanical strength to the materials [1, 2], and the biological components offer precise structural control and novel properties [3, 4]. These "smart" biohybrid materials with synergistic combination of functions possess high potential for biomedical applications such as drug delivery, tissue engineering, and biosensors [5, 6].

Recently, oligonucleotide-based hydrogels have drawn considerable attention because of the intrinsic advantages of utilizing nucleobases as biological binding motifs [7]. The Watson–Crick base pairing, *i.e.*, hydrogen bonding between A/T and C/G, produces highly programmable biomaterials [8, 9]. Over the years, a variety of artificial oligonucleotides with chemically-modified nonphosphodiester backbones have been synthesized [10]. In contrast to natural DNA and RNA, these oligos are not susceptible to hydrolytic (enzymatic) cleavage; thus, they are stable in the biological system and suitable for biomedical applications. Within the artificial oligos, the peptide nucleic acid (PNA) is of particular interest. PNAs are DNA analogs in which a 2-aminoethyl-glycine linkage replaces the phosphodiester backbone, and nucleobases are connected to this backbone at the amino nitrogens through a methylcarbonyl linker [11]. This peptide-like amide backbone is achiral, non-ionic, and relatively flexible, making PNA a much stronger binder than DNA (mainly due to lack of charge repulsion from phosphate). Interestingly, previous reports have shown that PNA is capable of sequence-specific binding to DNA, obeying the Watson-Crick pattern, to form a double helix [12, 13]. PNA may also recognize particular DNA sequences to generate other complex yet specific helical structures such as triplex or quadruplex [14–16]. For example, a unique "P-form" triple helix conformation

comprising two polypyrimidine PNAs and one polypurine DNA can be achieved *via* combination of Watson–Crick and Hoogsteen base interactions [14].

In this report, we present a new design of oligonucleotide-based hybrid hydrogels that employs the abovementioned PNA/DNA complexation to induce crosslinking of synthetic polymer chains, which leads to gelation. We demonstrate that the hydrogels can be formed due to two distinct types of complexations (Figure 1). The type I gel utilizes the PNA/DNA duplex hybridization, the Watson–Crick base pairing between two complementary sequences. The type II gel is formed *via* P-form oligonucleotide triplex composed of two homopyrimidine PNAs and one homopurine DNA. In these designs, the self-assembly of the "linker DNA" and the PNAs that are grafted to the polymer chains produces polymer networks expanded throughout the whole volume by water. This unique biorecognition/gelling process was mediated by oligonucleotide hybrids as macromolecular physical crosslinkers.

For the primary chain of hydrogels, we select synthetic, linear poly[*N*-(2-hydroxypropyl)methacrylamide] (polyHPMA), a hydrophilic and biocompatible polymer used extensively in drug delivery and tissue engineering [17–20]. Besides being chemically and hydrolytically stable, HPMA polymers exhibit physicochemical properties that mimic natural living tissues and possess a well-established safety profile in the human body [17, 18]. Previously, our laboratory showed that HPMA copolymers containing peptide grafts could trigger formation of hydrogels [3, 21–23]. These self-assembled hydrogels have become our inspiration for the design of a "drug-free" therapeutic system that crosslinks cell receptors and induces apoptosis of cancers [24–26]. Herein we present another self-assembling hybrid system utilizing PNA with potential for the further designs of novel nanomedicines.

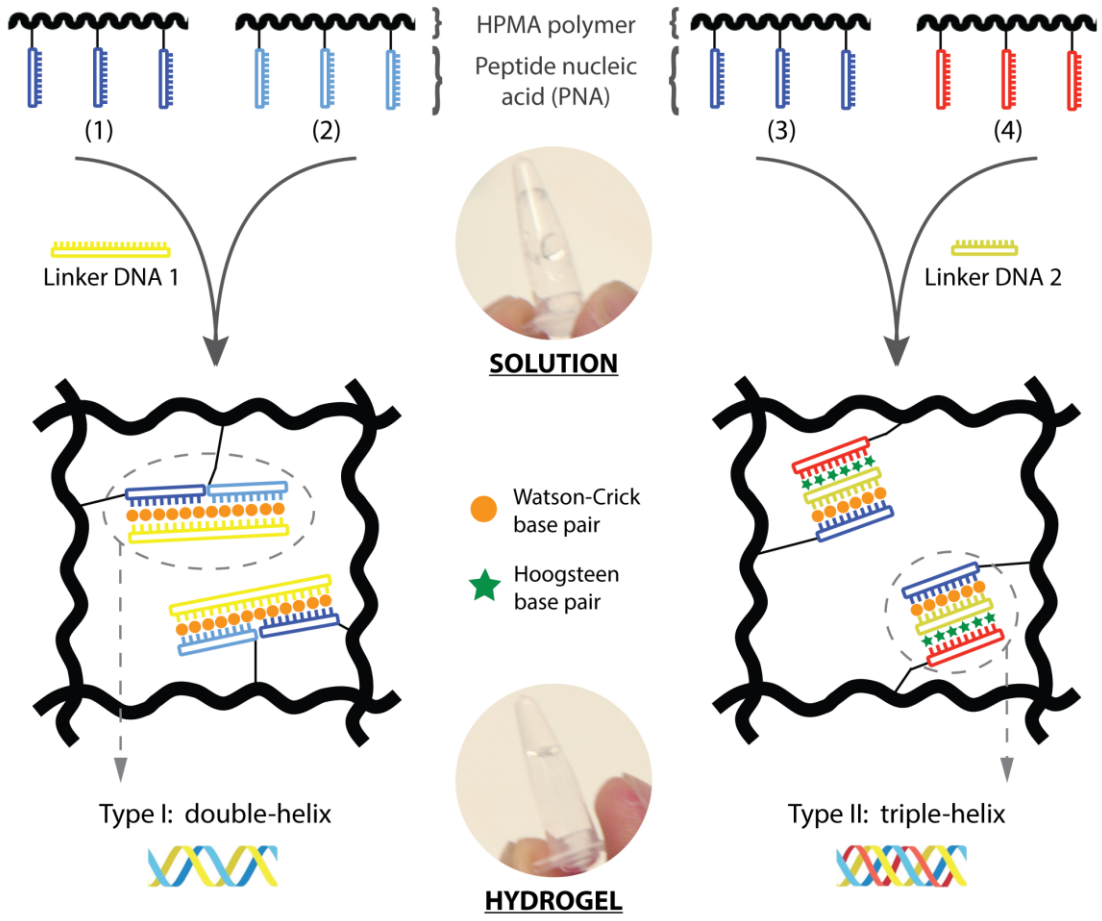

Figure 1. Hybrid hydrogels formed *via* PNA/DNA complexation. PNA sequences are grafted to linear HPMA polymer chains to produce multivalent conjugates (1) – (4). Upon addition of the linker DNAs, gelation occurs through the PNA/DNA duplex (type I) or the PNA_2/DNA triplex (type II).

2. Materials and Methods

2.1. Materials

Trityl chloride resin was purchased from P3 BioSystems (Shelbyville, KY). Fmoc-PNA-adenine(Bhoc)-OH, Fmoc-PNA-guanine(Bhoc)-OH, Fmoc-PNA-cytosine(Bhoc)-OH and Fmoc-PNA-thymine-OH were purchased from PolyOrg (Leominster, MA). *N,N,N′,N′*-Tetramethyl-*O*-(1*H*-benzotriazol-1-yl)uronium hexafluorophosphate (HBTU) was purchased from AAPPTec (Louisville, KY), and hydroxybenzotriazole (HOBT) from Novabiochem (San Diego, CA). *N,N*-Dimethylformamide (DMF), dichloromethane (DCM), methanol (MeOH), *N*-methylmorpholine

(NMM), *N*,*N*-diisopropylethylamine (DIPEA), trifluoroacetic acid (TFA), triisopropylsilane (TIS), pyridine, piperidine, acetone, diethyl ether and phenol were purchased from Sigma-Aldrich (St. Louis, MO). Acetic anhydride (Ac_2O) was purchased from Mallinckrodt Chemical Works (St. Louis, MO), and 2,6-lutidine from Promega (Madison, WI). 4,4′-Azobis(4-cyanopentanoic acid) (V-501) was purchased from Wako Chemicals (Richmond, VA). *N*-(2-Hydroxypropyl)methacrylamide (HPMA) [27], *N*-methacryloylglycylglycine (MA-GlyGly-OH) [28] and 4-cyanopentanoic acid dithiobenzoate (CPDB) [29] were synthesized as previously described. Linker DNAs (L-DNA1 and L-DNA2; for structures see Table 1) were ordered from the University of Utah Core Facility (Salt Lake City, UT).

Table 1. Base sequence and molecular weight (MW) of oligonucleotides.

Oligo #	Base Sequence / MW
MA-GlyGly-PNA1	MA-GlyGly-AGTGACCG-OH / 2391.9 Da
MA-GlyGly-PNA2	MA-GlyGly-ACCAGGCG-OH / 2376.9 Da
MA-GlyGly-PNA3	MA-GlyGly-TTCTCTTCTTC-OH / 3068.2 Da
MA-GlyGly-PNA4	MA-GlyGly-CTTCTTCTCTT-OH / 3068.2 Da
L-DNA1	5′-CGCCTGGTCGGTCACT-3′ / 4928.2 Da
L-DNA2	5′-GAAGAAGAGAA-3′ / 3526.3 Da

MA-GlyGly, methacryloyl-glycylglycine; L-DNA, linker DNA.

2.2. Solid-phase synthesis of polymerizable PNA

PNA oligo containing macromonomers (MA-GlyGly-PNA1, MA-GlyGly-PNA2, MA-GlyGly-PNA3, and MA-GlyGly-PNA4) were synthesized using manual Fmoc/tBu strategy on trityl chloride resin (Figure 2) following a protocol described by Avitabile *et al.* [30]. After swelling of the resin beads (200 mg, 0.21 mmol) in DCM (5 mL), the first PNA residue (0.06 mmol), dissolved in DMF, was attached to the resin in the presence of DIPEA. The rest of the

residues (0.15 mmol each), after deprotection with 20% piperidine (v/v) in DMF (2.5 mL), were dissolved in DMF/pyridine (3:2, vol %) and attached to the resin beads, one at a time, in the presence of HBTU (0.15 mmol), HOBT (0.15 mmol) and NMM (0.3 mmol). During synthesis, the completion of each coupling step was verified by Kaiser test. Each completed coupling was followed by a capping step with Ac_2O/lutidine/DMF (5:6:89, vol %) solution. After all the PNA residues were coupled, MA-GlyGly-OH (0.15 mmol) was attached to the N-terminus of oligos using the abovementioned coupling procedure. This process derivatized the PNA sequences with a polymerizable double bond (MA) *via* a glycine-glycine spacer, named MA-GlyGly-PNA. Resin-bound MA-GlyGly-PNA was cleaved with TFA/phenol/TIS (85:10:5, vol %) solution. Crude oligos were precipitated with cold diethyl ether, collected by centrifugation, dried in air, dissolved in double deionized (DI) water, and lyophilized. MA-GlyGly-PNA was purified and analyzed by reversed phase HPLC (Agilent Technologies, Santa Clara, CA) equipped with Zorbax 300SB-C18 column and eluted with double DI water and 0.1% TFA (v/v) (buffer A) and acetonitrile and 0.1% TFA (buffer B). Purified MA-GlyGly-PNA was confirmed by MALDI-ToF mass spectrometry (Voyager-DE STR Biospectrometry Workstation, PerSeptive Biosystems, Framingham, MA). Structures of MA-GlyGly-PNA1, MA-GlyGly-PNA2, MA-GlyGly-PNA3 and MA-GlyGly-PNA4 are shown in Table 1.

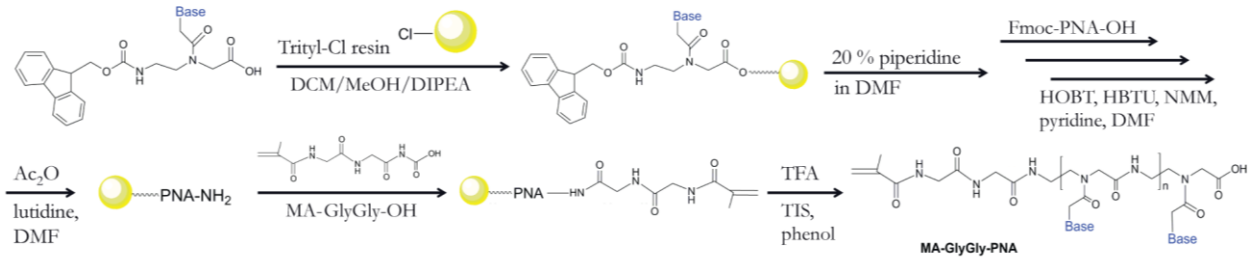

Figure 2. Schematic representation of the solid-phase synthesis of macromonomer MA-GlyGly-PNA. NMM, *N*-methylmorpholine; Ac_2O, acetic anhydride; TIS, triisopropylsilane.

2.3. Synthesis of polyHPMA grafted with PNA

The multivalent HPMA copolymer–PNA conjugates, named P–PNA1, 2, 3, or 4, were synthesized by reversible addition–fragmentation chain transfer (RAFT) polymerization. Macromonomers MA-GlyGly-PNA1, 2, 3, or 4, were used for copolymerization with HPMA. 4-Cyanopentanoic acid dithiobenzoate (CPDB) was used as the chain transfer agent, and V-501 as the initiator. A typical procedure was as follows: HPMA (28.3 mg, 0.198 mmol) and MA-GlyGly-PNA1 (4.8 mg, 0.002 mmol) were added into an ampoule attached to an Schlenk-line. After three vacuum/nitrogen cycles to remove oxygen, 0.1 mL degassed double DI water was added to dissolve the monomers, followed by addition of CPDB solution (0.07 mg in 15 μL methanol) and V-501 solution (0.02 mg in 20 μL methanol) *via* syringe. The mixture was bubbled with nitrogen for 5 min before sealing the ampoule; the copolymerization was performed at 70 °C for 18 h. The copolymer was isolated by precipitation into acetone and dried under vacuum overnight. P–PNA1 was purified by size exclusion chromatography (SEC) using ÄKTA FPLC with Sephacryl S-100 HR16/60 column (GE Healthcare, Pittsburgh, PA) eluted with sodium acetate buffer (pH 6.5) and 30% acetonitrile (v/v). Before injection to column, samples were dissolved in water and filtered through a 0.22 μm filter. After purification, samples were dialyzed against water extensively (1 kDa molecular weight cutoff) and freeze-dried overnight. Yield of the purified P–PNA1 was 16.2 mg (49%).

The copolymerization of HPMA with MA-GlyGly-PNA2, MA-GlyGly-PNA3, and MA-GlyGly-PNA4 is described in Supporting Information.

2.4. Characterization of P–PNA conjugates

P–PNA1, 2, 3, and 4, were characterized by UV absorbance at 265 nm using a Varian Cary 400 Bio UV–visible spectrophotometer (Agilent Technologies). Samples were placed in a 1

cm quartz cuvette for measurement. To quantify the content of PNA and determine the valence (number of oligos per polymer chain), the purified P–PNA conjugates were freeze-dried and dissolved in double DI water prior to UV–visible analysis. A molar absorptivity of 24,100 (M^{-1} cm^{-1}) was used for quantification of PNA1, 18,900 (M^{-1} cm^{-1}) for PNA2, and 108,000 (M^{-1} cm^{-1}) for PNA3 and PNA4. The molar absorptivities (extinction coefficients) were measured from the corresponding MA-GlyGly-PNA macromonomers. The valences of the P–PNA conjugates were calculated based on the resulting PNA contents and the molecular weights of the conjugates. The number average molecular weight (Mn), weight average molecular weight (Mw), and molecular weight distribution (polydispersity) of P–PNA were determined by SEC using ÄKTA FPLC with Superose 6 HR10/30 column (GE Healthcare) equipped with miniDAWN and OptilabREX detectors (GE Healthcare). The column was eluted with sodium acetate buffer (pH 6.5) and 30% acetonitrile (v/v) as the mobile phase.

2.5. Hydrogel preparation

Gels were obtained by, firstly, dissolving known amounts of lyophilized P–PNA conjugates in double DI water, and secondly, adding the linker DNA (L-DNA; dissolved in water) to the solution. To form hydrogels, P–PNA1 and P–PNA2 were paired with L-DNA1, and P–PNA3 and P–PNA4 with L-DNA2. The solution was vortexed thoroughly. Typically, the conjugate pairs were prepared at a concentration of 3 wt % or 5 wt %, and L-DNA was added with the ratio of 1:1 or 1:3 (PNA:DNA).

2.6. Microrheology

Particle-tracking passive microrheology analysis was performed following a protocol similar to one previously described [22]. P–PNA conjugates were weighed (~1 mg), placed in plastic Eppendorf tubes, and dissolved in predetermined amounts of water. Surfactant-free

yellow-green fluorescent amidine-modified polystyrene beads (Interfacial Dynamics, Portland, OR), 0.52 μm in diameter, were dispersed thoroughly into the solution, followed by the addition of L-DNA. Samples were immediately sealed between a microscope slide with melted parafilm and a No. 1.5 glass coverslip and then observed under a Nikon Eclipse E800 microscope equipped with a 100× oil-immersion objective. The Brownian motion of the fluorescent beads was visualized by a Dage-MTI DC330 CCD camera. For each sample, two thousand consecutive images were recorded using StreamPix software (Norpix, Montreal, Canada) at intervals of 33 ms. Images were analyzed by IDL software (Research Systems, Boulder, CO), and the trajectories of the particles were extracted and analyzed using the algorithms developed by Crocker *et al.* [31].

2.7. Scanning electron microscopy (SEM)

Hydrogel samples (1 mg; 5 wt % P–PNA, DNA:PNA=1:1), prepared as explained above, were fully swelled in UltraPure™ DNase/RNase-free distilled water (Life Technologies, Carlsbad, CA) overnight, followed by shock-freezing in liquid nitrogen and then lyophilization. The freeze-dried samples were carefully fractured and gathered on SEM aluminum stubs and sputtered with gold for 30 sec to obtain a conductive coating visible by SEM. The observation of the hydrogels morphology at the surface, as well as in bulk, was carried out on an FEI Quanta 600F Environmental SEM at an accelerating voltage of 15 kV and magnifications from 100 to 5000 times. Images were captured and processed under an FEI xT Microscopic Control software.

3. Results and Discussion

3.1. Synthesis of multivalent HPMA copolymer–PNA conjugates

HPMA copolymers grafted with multiple PNA oligos (P–PNA) were synthesized by RAFT copolymerization of HPMA with MA-GlyGly-PNA1, 2, 3, or 4 (Figure 3A). Polymerizable PNA containing a methacryloyl (MA) group was synthesized by a solid-phase synthesis approach (Figure 2) and used as a macromonomer for copolymerization with HPMA. Successful synthesis of the MA-GlyGly-PNA monomers was confirmed by HPLC (Figure S1) and mass spectroscopy (Figures S2–5). The nucleobase sequences of the PNAs and the linker DNAs are shown in Table 1. Copolymerizations of HPMA and MA-GlyGly-PNA1, MA-GlyGly-PNA2, MA-GlyGly-PNA3 and MA-GlyGly-PNA4, respectively, were carried out under identical conditions, which produced the multivalent conjugates P–PNA1, P–PNA2, P–PNA3 and P–PNA4 with similar physicochemical properties (Table 2). The conjugates were analyzed by UV–visible spectroscopy (Figure 3B); PNA grafts were characterized by absorbance at 265 nm. The results showed that each abovementioned P–PNA conjugate contained about 5 oligos per polymer chain. To compare the efficiency of hydrogel formation, we further prepared a pair of "low-valence" conjugates (P–PNA3a and P–PNA4a) that contained about 2 oligos per polymer chain. The syntheses of conjugates P–PNA3a and P–PNA4a were achieved by feeding half the amount of MA-GlyGly-PNA (1 mol %) during RAFT polymerization when compared to P–PNA3 and P–PNA4, which used 2 mol % MA-GlyGly-PNA in the feed. The PNAs were attached to the polymers *via* a glycine-glycine dipeptide spacer (to avoid steric hindrance of the polymer on oligo hybridization). The molecular weight (MW) and MW distribution of conjugates were analyzed by size exclusion chromatography (Figure 3C). As shown in Table 2, monodisperse polymer conjugates (polydispersity index $\leq$ 1.16) having similar MW (~100 kDa)

were reproducibly synthesized. Comparison between the high-valence conjugate pair (P–PNA3, P–PNA4) and the low-valence one (P–PNA3a, P–PNA4a) further indicated that the proposed one-pot synthetic process utilizing polymerizable MA-GlyGly-PNA was well controlled. All the P–PNA conjugates synthesized here were found to be water-soluble.

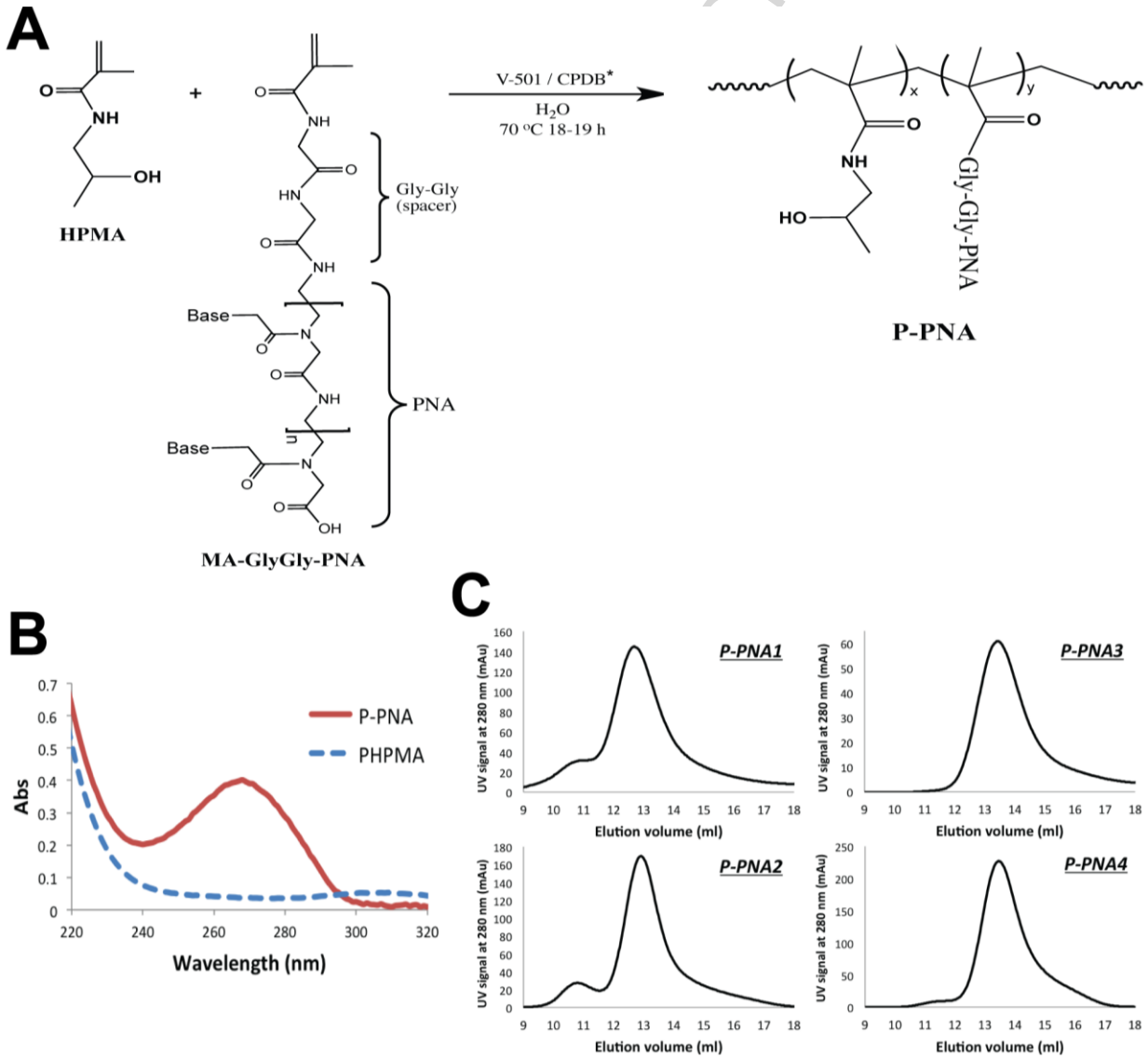

Figure 3. Synthesis and characterization of multivalent conjugate poly[HPMA-*co*-(MA-GlyGly-PNA)] (P–PNA). (A) RAFT polymerization of P–PNA. *CPDB, 4-cyanopentanoic acid dithiobenzoate (chain transfer agent). (B) UV–vis spectra of P–PNA and HPMA polymer (PHPMA). (C) Size exclusion chromatography of P–PNA conjugates. Superose 6 HR10/30 column was eluted with sodium acetate buffer and 30% acetonitrile (v/v). See Table 1 for structures of PNAs.

Table 2. Characterization of multivalent P–PNA conjugates.

Conjugate #	Mn[a] (kDa)	Mw[b] (kDa)	PDI[c] (kDa)	Valence[d]
P–PNA1	115.2	130.6	1.13	5.6
P–PNA2	94.5	107.6	1.14	5.5
P–PNA3	117.4	131.1	1.12	5.4
P–PNA4	91.7	96.0	1.05	4.9
P–PNA3a	81.0	89.8	1.11	2.4
P–PNA4a	95.2	110.1	1.16	2.3

[a] Number average molecular weight; determined by size exclusion chromatography (SEC).
[b] Weight average molecular weight; determined by SEC.
[c] Polydispersity index (PDI); PDI = Mw/Mn.
[d] Number of PNA grafts per polymer chain; determined by UV–vis spectroscopy.

3.2. Hybrid polymeric hydrogels formed via PNA/DNA complexation

To prepare hydrogels, the conjugate pairs were dissolved in water, followed by addition of the corresponding linker DNA (L-DNA). L-DNA1 having a Watson–Crick complementary sequence to PNA1 plus PNA2 was added to the P–PNA1/P–PNA2 solution to form the type I "double-helix" gel. To prepare the type II "triple-helix" hydrogel, the homopurine L-DNA2, capable of forming a P-form triplex with the homopyrimidine PNA3 and PNA4, was used along with conjugates P–PNA3 and P–PNA4 (or P–PNA3a and P–PNA4a). The initial results by visual observation suggested that, for the conjugates containing 5 PNAs per polymer chain and prepared at a 5 wt % concentration, gelation occurs within minutes after the addition of linker DNAs, whereas solutions at the same concentration but prepared from the conjugates containing 2 PNAs per polymer chain gelled after incubation for several hours at room temperature. This observation indicated that the PNA graft density or the number of physical crosslinking points on the polymer backbone was influential on the gelation process, as previously reported for the hydrogels self-assembled from HPMA copolymers containing peptide grafts [21–23]. Increasing

the valence of the designed conjugates would result in faster gelation kinetics, increased crosslinking density, and, consequently, stronger mechanical properties of the gels.

The self-assembly of the hydrogels is mediated by biorecognition of the complementary moieties. When P–PNA1 + P–PNA2 was mixed with non-specific linker DNA2, the hydrogel did not form. Similarly, when P–PNA3 + P–PNA4 was mixed with non-specific linker DNA1, the gelation did not occur either (see Supporting Information).

Interestingly, we observed a shear-thinning property on both type I and type II hydrogels. Applying mechanical forces, *e.g.*, vortex or agitation, resulted in disassembly of the metastable hydrogel structure and dissolution of the polymer networks, after which, the gels could be easily reassembled by standing at room temperature. This thixotropic phenomenon was previously observed in our laboratory on hybrid hydrogels self-assembled from HPMA copolymers grafted with β-sheet peptides [23]. As macromolecular physical crosslinkers, oligonucleotides and β-sheet peptides share similar characteristics, as hydrogen bonding is the dominant driving force for both conformations. Previous research has shown that, utilizing hydrogen bonding, it is possible to construct highly sensitive pH-responsive hydrogels [32–34]. For example, Willner and colleagues designed a pH-stimulated DNA hydrogel that exhibited a unique shape-memory property [32]. These hybrid functional materials with "switchable" nature have great potential for applications such as biosensing, separation and purification of nuclei acids, and controlled release [7–9].

3.3. Microrheology of type I (double-helix) hydrogel

The gelation behavior of P–PNA upon addition of L-DNA was characterized by microrheology. The Brownian motion of small tracer particles embedded into the samples was analyzed using algorithms previously developed [31]. The averaged mean square displacement

(MSD) of the particles as a function of lag time (tau) was calculated based on the extracted trajectories. The double logarithmic plot of MSD versus tau allows one to determine the viscoelastic property of the sample [23, 31]. In a viscous fluid (*i.e.*, solution), the particles can diffuse freely and the Brownian motion causes a linear MSD–tau relationship with a slope of 1. In an elastic system (*i.e.*, hydrogel), the particle movement is constrained and the slope of the MSD–tau curve is 0. Figure 4A shows the microrheology analysis of the type I (duplex) hydrogel. The aqueous solution of P–PNA1 and P–PNA2 (without linker DNA) demonstrated a viscous fluid characteristic where linear dependence of MSD with lag time was observed. Immediately after the addition of L-DNA1, the solution was rendered elastic (or viscoelastic) as indicated by no (or limited) Brownian motion of the tracer particles. When the solution was prepared at 3 wt % P–PNA followed by an equimolar concentration of DNA/PNA, we observed small MSD growth with tau and limited fluctuation of MSD amplitude at shorter lag times. This is indicative of a partially viscoelastic, gel-like environment. Such a viscoelastic intermediate phenomenon has been previously reported for other hybrid hydrogels [35–37]. Importantly, when a higher concentration of P–PNA (5 wt %) or an excess amount of L-DNA (3×) was used, the MSD reached a plateau over lag time, indicating largely elastic hydrogels formed *via* PNA/DNA hybridization.

The microrheology measurements also allowed to quantify the mechanical properties of the hybrid hydrogels. The elastic or storage modulus (G′) and the viscous or loss modulus (G″) of the samples were calculated as a function of the Laplace frequency using the modified Stokes−Einstein equation [38]. The results (Figures 4B–D) corresponded well with the MSD data and showed that type I hydrogels could be achieved at a concentration of 5 wt % P–PNA or by using a 3× excess L-DNA1 at 3 wt % P–PNA. In the control sample, *i.e.*, aqueous solution of

P–PNA1 and P–PNA2 (without linker DNA), G′ was very close to zero and could not be calculated and G″ significantly exceeded G′ (Figure S6). This indicated a largely viscous environment. In the hydrogel samples (Figures 4C and D), G′ was insensitive to frequency and showed a plateau-like behavior and was significantly larger than G″ at higher frequencies. The double logarithmic plots of viscoelastic moduli versus frequency showed a crossover or the tendency of a crossover between G′ and G″, another indicator for hydrogel formation [37, 38]. These hydrogels had a crossover frequency of about 0.2 rad/sec. The elastic modulus of the 5%, 1:1 gel (Figure 4D) was substantially larger than that of the 3%, 1:3 gel (Figure 4C). In Figure 4B, the solution of 3 wt % P–PNA with addition of an equimolar DNA was viscoelastic. There was no crossover point between G′ and G″ in the frequency-dependent plots and G′ was only slightly larger than G″, suggesting the transition from a viscous medium to a hydrogel under the applied condition [23]. In conjunction these results suggested a critical concentration at about 3 wt % polymer conjugate for the formation of type I double-helix mediated hydrogel. Increasing the concentration of P–PNA or linker DNA could both produce hybrid hydrogels that displayed largely elastic behavior.

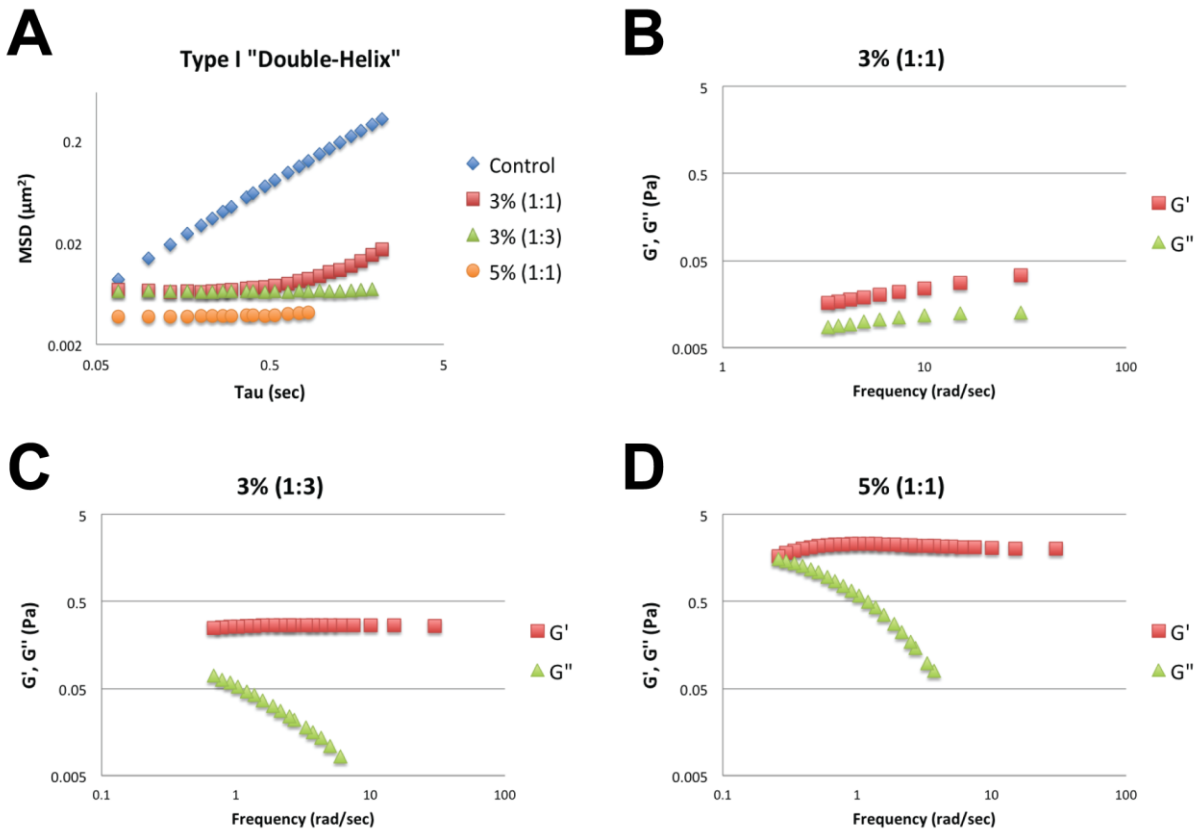

Figure 4. Microrheology and viscoelastic analysis of "type I" (duplex) hydrogel. (A) Mean square displacement (MSD) as a function of lag time (tau). *Control*, 5 wt % P–PNA1 + P–PNA2 in water (without linker DNA); *3% (1:1)*, 3 wt % P–PNA1 + P–PNA2 with equimolar L-DNA1; *3% (1:3)*, 3 wt % P–PNA1 + P–PNA2 with 3× excess L-DNA1; *5% (1:1)*, 5 wt % P–PNA1 + P–PNA2 with equimolar L-DNA1. (B) (C) (D) Frequency-dependent linear viscoelastic moduli at different concentrations of conjugates. G′, storage modulus; G″, loss modulus. Experiments were performed at 3 h after mixing the samples, using conjugates with valence = 5.

The approach of hydrogel formation *via* hybridization (double-helix) of oligonucleotides derivatized in water-soluble polymers was firstly reported by Nagahara and Matsuda [39]. Over the decades, numerous designs have emerged in this rapidly developing field [40–46]. These designs utilized the binding effect of natural DNA or RNA for applications such as (i) controlled or triggered release of therapeutic nucleic acids [41], (ii) separation or detection of environmental DNA [43, 44], and (iii) sensing or removal of hazardous metals (*i.e.*, employing specific binding between nucleobases and metal ions) [45, 46]. However, DNA and RNA are

notoriously susceptible to enzymatic degradation, which disables these previous designs for further applications in the biological system. In this report, we exploit hybrid hydrogels formation from synthetic PNA oligonucleotides that are stable in the body. The proposed material system is suitable for broad pharmaceutical applications.

3.4. Microrheology of type II (triple-helix) hydrogel

The gelation process of the type II P-form triplex mediated design was studied by microrheology (Figure 5). As shown in Figure 5A, the control sample, *i.e.*, aqueous solution of P–PNA3 and P–PNA4 (without linker DNA), possessed a largely viscous characteristic where the slope of the MSD–tau curve was 1. We firstly analyzed the sample at 3 wt % polymer conjugate with an equimolar L-DNA, the viscoelastic intermediate condition for type I hydrogel. Unlike the type I gel, the data here showed no dependence of MSD with lag time (slope = 0), a purely elastic characteristic. When the sample was further tested at 5 wt % P–PNA with an equimolar L-DNA2, a similar MSD profile was obtained. These results indicated a lower critical gelation concentration (below 3 wt %) for the triple-helix mediated hydrogel when compared to the double-helix design. Such difference can potentially be explained by (i) stronger binding of the triplex conformation and (ii) faster diffusion of the smaller L-DNA2 (11 mer) in solution when compared to L-DNA1 (16 mer).

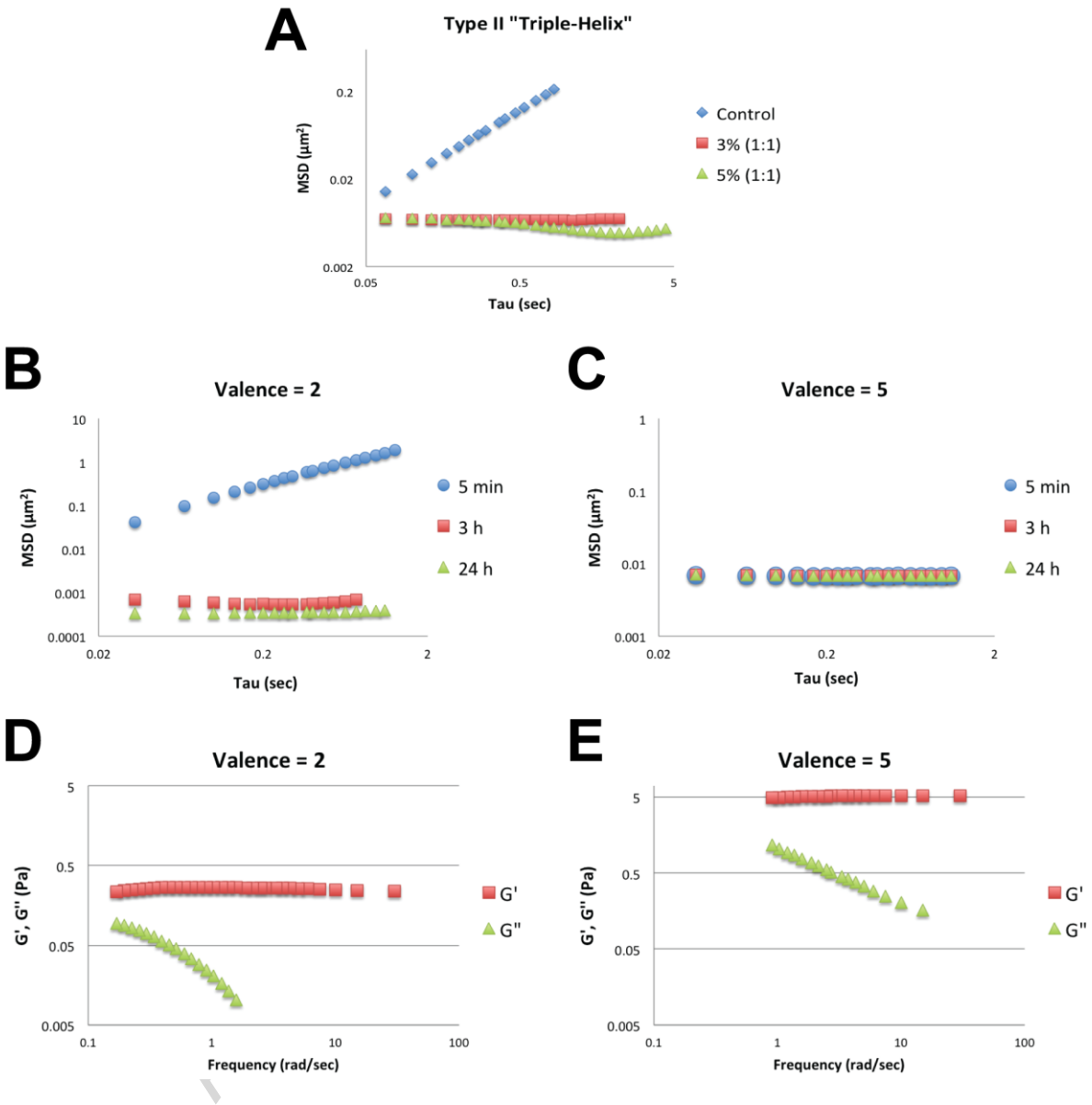

Figure 5. Microrheology and viscoelastic analysis of "type II" (triplex) hydrogel. (A) Mean square displacement (MSD) as a function of lag time (tau). *Control*, 5 wt % P–PNA3 + P–PNA4 in water (without linker DNA); *3% (1:1)*, 3 wt % P–PNA3 + P–PNA4 with equimolar L-DNA2; *5% (1:1)*, 5 wt % P–PNA3 + P–PNA4 with equimolar L-DNA2. Valence of conjugates was 5. (B) (C) MSD vs. tau at different times after mixing L-DNA2 with conjugates (valence = 2 or 5). (D) (E) Frequency-dependent linear viscoelastic analysis. G′, storage modulus; G″, loss modulus. Experiments were performed at 3 h after mixing the samples, unless otherwise indicated.

The type II hydrogel was further analyzed at 3 wt % polymer conjugate (Figures 5B–E). We compared the low-valence conjugate pair (P–PNA3a, P–PNA4a) with the high-valence one (P–PNA3, P–PNA4) to study the impact of PNA graft density on gelation. Characterization of

MSD (Figures 5B and C) demonstrated different gelation kinetics between the low- and high-valence conjugates. As shown in Figure 5C, the conjugates containing 5 PNAs per polymer chain gelled almost immediately (< 5 min) upon addition of the linker DNA. In contrast, for P–PNA3a and P–PNA4a, both having a valence of 2, gelation did not occur right after adding L-DNA (Figure 5B). However, when the analysis was performed at 3 h after incubation in room temperature, the MSD reached a plateau over lag time, indicating hydrogel formation. For further comparison, the viscoelastic moduli of type II hydrogels formed from the high- and low-valence conjugates were determined at 3 h (Figures 5D and E). Both samples demonstrated largely elastic nature. Interestingly, the elastic modulus (G′) of the high-valence gel was over one degree of magnitude larger than that of the low-valence gel, suggesting increased stiffness of the material at a higher crosslinking density. These data in conjunction indicated the possibility of producing more rigid hydrogels by designing greater number of crosslinking points on the polymer chain.

Hydrogel formation mediated by the oligonucleotide triplex is a new concept. Recently, Ren *et al.* reported a DNA triplex-crosslinked hydrogel system that was pH-labile [34]. The designed triple helix bound specifically to an anticancer drug, coralyne (*i.e.*, intercalation into the TA•T triplex), and the pH-controlled release of the drug from the hydrogel was demonstrated. Here, utilizing non-degradable PNA, we present yet another novel method for the preparation of Hoogsteen triplex-based hydrogels. The gelation is triggered by the unique PNA_2/DNA (P-form) conformation [14], and the hydrogel is enzymatically stable and suitable for applications in the biological system.

3.5. Morphology of hybrid hydrogels

Scanning electron microscopy (SEM) was used to visualize the microstructure of the hydrogels. The two types of hydrogels were both prepared at 5 wt % P–PNA with an equimolar L-DNA for comparison. Before the imaging, the samples were shock-frozen with liquid nitrogen, lyophilized, and then coated with gold. This procedure had minimal impact on the hydrogel structure [47]. As shown in Figure 6, the porous structure is most probably interconnected in both types of gels (results were obtained from more than ten images for each gel type from different angles and with varying magnifications). Such structures are typical for physically crosslinked polymer networks [32, 42, 47]. Interestingly, we observed substantially different pore sizes between the two types of hydrogels. The type I double-helix hydrogel contained a more open structure with larger pore sizes (about 80–100 μm diameter), whereas the type II triplex hydrogel displayed a denser structure exhibiting significantly smaller pore sizes (below 5 μm). This observation is in agreement with the microrheology data where the type I gel had a higher critical gelation concentration and potentially a greater stiffness. Coherently, these results suggest a more rigid conformation of the triplex-crosslinked hydrogel when compared to the double-helix design. These microporous materials have potential as drug and gene delivery vehicles [34, 41], tissue engineering scaffolds [19, 20] and in sensors and actuators [6–9]. Similarly to calmodulin-based hydrogels [48], these hydrogels could be used as valves in microfluidic devices. Biorecognition mediated changes in the degree of swelling [4, 48] would open or close a valve in the microfluidic channel.

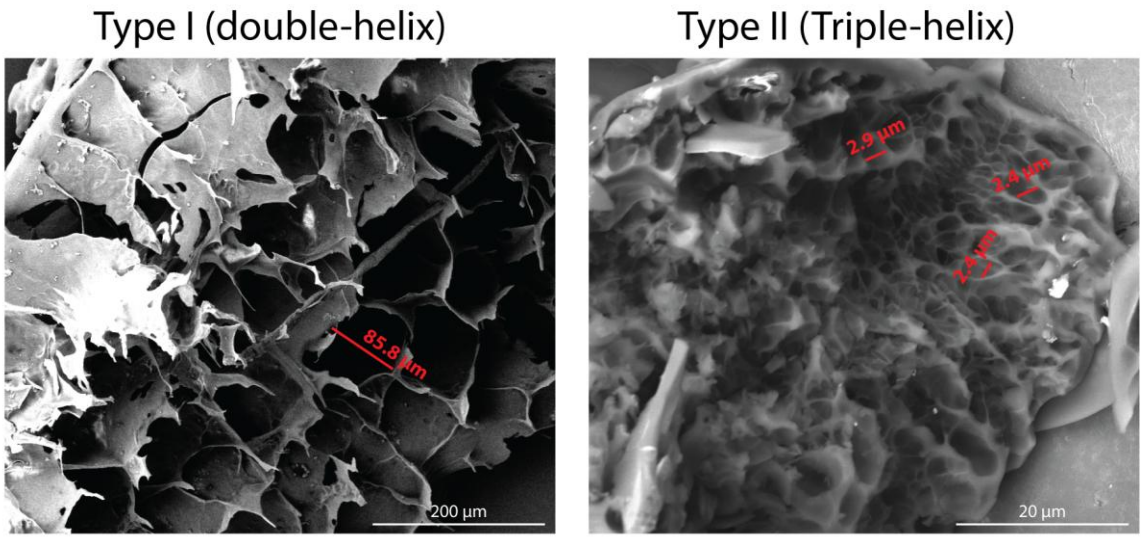

Figure 6. Freeze-dried SEM images of the two types of hydrogels. Both samples were prepared at 5 wt % P–PNA with an equimolar L-DNA.

4. Conclusions

The present study has introduced new methods to synthesize water-soluble polymer/PNA hybrid hydrogels. HPMA copolymers grafted with multiple PNA oligos (P–PNA) have been synthesized by RAFT polymerization where polymerizable PNA containing a methacryloyl group (MA-GlyGly-PNA) has been used as a macromonomer. By the appropriate design of the base sequences, hydrogel formation has been achieved by adding corresponding linker DNAs to the P–PNA solutions. We have demonstrated the successful gelations from the two distinct designs. Type I hydrogel utilizes the PNA/DNA double-helix hybridization. Type II hydrogel is formed *via* P-form oligonucleotide triplex composed of two homopyrimidine PNAs and one homopurine DNA. Microrheology has further confirmed the gelations and has revealed a lower critical gelation concentration (below 3 wt %) for the triplex-mediated hydrogel when compared to the double-helix design (at 3 wt %). We have further shown the possibility of producing more rigid hydrogels by designing higher crosslinking densities (*i.e.*, greater number of PNA grafts on

the polymer chain). Finally, SEM imaging has shown that the type I hydrogel exhibits larger pore sizes than the type II hydrogel; both are interconnected microporous materials.

This work has explored the possibility of novel hydrogels formation based on PNA/DNA complexation. The proposed approach has generated polymeric networks that display relatively weak mechanical properties due to the physical crosslinking (*i.e.*, hydrogen bonding). This is a new paradigm of hybrid hydrogels self-assembled from synthetic water-soluble graft copolymers. Previously, our laboratory pioneered the design of hybrid polymeric hydrogels crosslinked by coiled-coil protein domains [3]. Such design became our inspiration for a cell surface receptor crosslinking-mediated therapeutic system that induced apoptotic cell death of cancers [24, 25]. Here, we have presented yet another self-assembling material system utilizing oligonucleotides complexation. The concept established in this study can potentially be applied into new "drug-free" therapeutics design [26].

Acknowledgments

This work was supported in part by NIH grant GM95606 from the National Institute of General Medical Sciences (to J.K.) and the University of Utah Undergraduate Research Opportunity Program (to J.F.). The authors thank Dr. Paulo Perez and the Utah Nanofab at the University of Utah for assisting with SEM imaging.

References

[1] J. Li, W.R. Illeperuma, Z. Suo, J.J. Vlassak, Hybrid hydrogels with extremely high stiffness and toughness, ACS Macro Lett. 3 (2014) 520–523.

[2] X. Wang, H. Wang, H.R. Brown, Jellyfish gel and its hybrid hydrogels with high mechanical strength, Soft Matter 7 (2011) 211–219.

[3] C. Wang, R.J. Stewart, J. Kopec□ek, Hybrid hydrogels assembled from synthetic polymers and coiled-coil protein domains, Nature 397 (1999) 417–420.

[4] W. Yuan, J. Yang, P. Kopec□ková, J. Kopec□ek, Smart hydrogels containing adenylate kinase: translating substrate recognition into macroscopic motion, J. Am. Chem. Soc. 130 (2008) 15760–15761.

[5] N. Hotz, L. Wilcke, W. Weber, Design, synthesis, and application of stimulus-sensing biohybrid hydrogels, Macromol. Rapid Commun. 34 (2013) 1594–1610.

[6] J. Kopeček, J. Yang, Smart self-assembled hybrid hydrogel biomaterials, Angew. Chem. Int. Ed. 51 (2012) 7396–7417.

[7] X. Xiong, C. Wu, C. Zhou, G. Zhu, Z. Chen, W. Tan, Responsive DNA-based hydrogels and their applications, Macromol. Rapid Commun. 34 (2013) 1271–1283.

[8] M.R. Jones, N.C. Seeman, C.A. Mirkin, Nanomaterials. Programmable materials and the nature of the DNA bond, Science 347 (2015) 1260901.

[9] Z.G. Wang, B. Ding, DNA-based self-assembly for functional nanomaterials, Adv. Mater. 25 (2013) 3905–3914.

[10] P.E. Nielsen, DNA analogues with nonphosphodiester backbones, Annu. Rev. Biophys. Biomol. Struct. 24 (1995) 167–183.

[11] M. Egholm, O. Buchardt, P.E. Nielsen, R.H. Berg, Peptide nucleic acids (PNA). Oligonucleotide analogs with an achiral peptide backbone, J. Am. Chem. Soc. 114 (1992) 1895–1897.

[12] M. Egholm, O. Buchardt, L. Christensen, C. Behrens, S.M. Freier, D.A. Driver, R.H. Berg, S.K. Kim, B. Nordén, P.E. Nielsen, PNA hybridizes to complementary oligonucleotides obeying the Watson–Crick hydrogen-bonding rules, Nature 365 (1993) 566–568.

[13] P. Wittung, P.E. Nielsen, O. Buchardt, M. Egholm, B. Nordén, DNA-like double helix formed by peptide nucleic acid, Nature 368 (1994) 561–563.

[14] L. Betts, J.A. Josey, J.M. Veal, S.R. Jordan, A nucleic acid triple helix formed by a peptide nucleic acid–DNA complex, Science 270 (1995) 1838–1841.

[15] M. Egholm, P.E. Nielsen, O. Buchardt, R.H. Berg, Recognition of guanine and adenine in DNA by cytosine and thymine containing peptide nucleic acids (PNA), J. Am. Chem. Soc. 114 (1992) 9677–9678.

[16] T. Ishizuka, J. Yang, M. Komiyama, Y. Xu, G-rich sequence-specific recognition and scission of human genome by PNA/DNA hybrid G-quadruplex formation, Angew. Chem. Int. Ed. 51 (2012) 7198–7202.

[17] J. Kopec□ek, P. Kopec□ková, HPMA copolymers: origins, early developments, present, and future, Adv. Drug Deliv. Rev. 62 (2010) 122–149.

[18] K. Ulbrich, V. Šubr, Structural and chemical aspects of HPMA copolymers as drug carriers, Adv. Drug Deliv. Rev. 62 (2010) 150–166.

[19] S.M. Choi, D. Singh, Y.W. Cho, T.H. Oh, S.S. Han, Three-dimensional porous HPMA-*co*-DMAEM hydrogels for biomedical application, Colloid Polym. Sci. 291 (2013) 1121–1133.

[20] A. Hejc□l, J. Sedý, M. Kapcalová, D.A. Toro, T. Amemori, P. Lesný, K. Likavcanová-Mašínová, E. Krumbholcová, M. Přádný, J. Michálek, M. Burian, M. Hájek, P. Jendelová, E. Syková, HPMA-RGD hydrogels seeded with mesenchymal stem cells improve functional outcome in chronic spinal cord injury, Stem Cells Dev. 19 (2010) 1535–1546.

[21] J. Yang, C. Xu, C. Wang, J. Kopec□ek, Refolding hydrogels self-assembled from HPMA graft copolymers by antiparallel coiled-coil formation, Biomacromolecules 7 (2006) 1187–1195.

[22] J. Yang, C. Xu, P. Kopec□ková, J. Kopec□ek, Hybrid hydrogels self-assembled from HPMA copolymers containing peptide grafts, Macromol. Biosci. 6 (2006) 201–209.

[23] L.C. Radu-Wu, J. Yang, K. Wu, J. Kopec□ek, Self-assembled hydrogels from poly[*N*-(2-hydroxypropyl)methacrylamide] grafted with beta-sheet peptides, Biomacromolecules 10 (2009) 2319–2327.

[24] K. Wu, J. Liu, R.N. Johnson, J. Yang, J. Kopeček, Drug-free macromolecular therapeutics: induction of apoptosis by coiled-coil-mediated cross-linking of antigens on the cell surface, Angew. Chem. Int. Ed. 49 (2010) 1451–1455.

[25] K. Wu, J. Yang, J. Liu, J. Kopeček, Coiled-coil based drug-free macromolecular therapeutics: *in vivo* efficacy, J. Controlled Release 157 (2012) 126–131.

[26] T.-W. Chu, J. Kopeček, Drug-free macromolecular therapeutics – a new paradigm in polymeric nanomedicines, Biomater. Sci. 3 (2015) 908–922.

[27] J. Kopeček, H. Bažilová, Poly[*N*-(2-hydroxypropyl)methacrylamide] – I. Radical polymerization and copolymerization, Eur. Polym. J. 9 (1973) 7–14.

[28] J. Drobník, J. Kopeček, J. Labský, P. Rejmanová, J. Exner, V. Saudek, J. Kálal, Enzymatic cleavage of side chains of synthetic water-soluble polymers, Makromol. Chem. 177 (1976) 2833–2848.

[29] Y. Mitsukami, M.S. Donovan, A.B. Lowe, C.L. McCormick, Water-soluble polymers. 81. Direct synthesis of hydrophilic styrenic-based homopolymers and block copolymers in aqueous solution *via* RAFT, Macromolecules 34 (2001) 2248–2256.

[30] C. Avitabile, L. Moggio, L.D. D'Andrea, C. Pedone, A. Romanelli, Development of an efficient and low-cost protocol for the manual PNA synthesis by Fmoc chemistry, Tetrahedron Lett. 51 (2010) 3716–3718.

[31] J.C. Crocker, M.T. Valentine, E.R. Weeks, T. Gisler, P.D. Kaplan, A.G. Yodh, D.A. Weitz, Two-point microrheology of inhomogeneous soft materials, Phys. Rev. Lett. 85 (2000) 888–891.

[32] W. Guo, C.H. Lu, R. Orbach, F. Wang, X.J. Qi, A. Cecconello, D. Seliktar, I. Willner, pH-stimulated DNA hydrogels exhibiting shape-memory properties, Adv. Mater. 27 (2015) 73–78.

[33] W. Guo, C.H. Lu, X.J. Qi, R. Orbach, M. Fadeev, H.H. Yang, I. Willner, Switchable bifunctional stimuli-triggered poly-*N*-isopropylacrylamide/DNA hydrogels, Angew. Chem. Int. Ed. 53 (2014) 10134–10138.

[34] J. Ren, Y. Hu, C.-H. Lu, W. Guo, M.A. Aleman-Garcia, F. Ricci, I. Willner, pH-responsive and switchable triplex-based DNA hydrogels, Chem. Sci. 6 (2015) 4190–4195.

[35] W.A. Petka, J.L. Harden, K.P. McGrath, D. Wirtz, D.A. Tirrell, Reversible hydrogels from self-assembling artificial proteins, Science 281 (1998) 389–392.

[36] K. Dooley, B. Bulutoglu, S. Banta, Doubling the cross-linking interface of a rationally designed beta roll peptide for calcium-dependent proteinaceous hydrogel formation, Biomacromolecules 15 (2014) 3617–3624.

[37] K. Dooley, Y.H. Kim, H.D. Lu, R. Tu, S. Banta, Engineering of an environmentally responsive beta roll peptide for use as a calcium-dependent cross-linking domain for peptide hydrogel formation, Biomacromolecules 13 (2012) 1758–1764.

[38] T.G. Mason, D.A. Weitz, Optical measurements of frequency-dependent linear viscoelastic moduli of complex fluids, Phys. Rev. Lett. 74 (1995) 1250–1253.

[39] S. Nagahara, T. Matsuda, Hydrogel formation *via* hybridization of oligonucleotides derivatized in water-soluble vinyl polymers, Polym. Gels Netw. 4 (1996) 111–127.

[40] F.E. Alemdaroglu, A. Herrmann, DNA meets synthetic polymers - highly versatile hybrid materials, Org. Biomol. Chem. 5 (2007) 1311–1320.

[41] X. Zhang, M.R. Battig, Y. Wang, Programmable hydrogels for the controlled release of therapeutic nucleic acid aptamers *via* reversible DNA hybridization, Chem. Commun. 49 (2013) 9600–9602.

[42] G. Sicilia, C. Grainger-Boultby, N. Francini, J.P. Magnuson, A.O. Saeed, F. Fernández-Trillo, S.G. Spain, C. Alexander, Programmable polymer-DNA hydrogels with dual input and multiscale responses, Biomater. Sci. 2 (2014) 203–211.

[43] S. Tierney, B.T. Stokke, Development of an oligonucleotide functionalized hydrogel integrated on a high-resolution interferometric readout platform as a label-free macromolecule sensing device, Biomacromolecules 10 (2009) 1619–1626.

[44] Y. Murakami, M. Maeda, Hybrid hydrogels to which single-stranded (ss) DNA probe is incorporated can recognize specific ssDNA, Macromolecules 38 (2005) 1535–1537.

[45] N. Dave, M.Y. Chan, P.J. Huang, B.D. Smith, J. Liu, Regenerable DNA-functionalized hydrogels for ultrasensitive, instrument-free mercury(II) detection and removal in water, J. Am. Chem. Soc. 132 (2010) 12668–12673.

[46] H. Lin, Y. Zou, Y. Huang, J. Chen, W.Y. Zhang, Z. Zhuang, G. Jenkins, C.J. Yang, DNAzyme crosslinked hydrogel: a new platform for visual detection of metal ions, Chem. Commun. 47 (2011) 9312–9314.

[47] C. Xu, V. Breedveld, J. Kopeček, Reversible hydrogels from self-assembling genetically engineered protein block copolymers, Biomacromolecules 6 (2005) 1739–1749.

[48] J.D. Ehrick, S.K. Deo, T.W. Browning, L.G. Bachas, M.J. Madou, S. Daunert, Genetically engineered protein in hydrogels tailors stimuli-responsive characteristics, Nature Mater. 4 (2005) 298–302.